Virology ▮ (▮▮▮▮) ▮▮▮–▮▮▮

Contents lists available at SciVerse ScienceDirect

Virology

journal homepage: www.elsevier.com/locate/yviro

In vivo subcellular localization of *Mal de Río Cuarto virus* (MRCV) non-structural proteins in insect cells reveals their putative functions

Guillermo A. Maroniche, Vanesa C. Mongelli, Gabriela Llauger, Victoria Alfonso, Oscar Taboga, Mariana del Vas*

Instituto de Biotecnología, CICVyA, Instituto Nacional de Tecnología Agropecuaria (IB-INTA), Las cabañas y Los Reseros s/n. Hurlingham Cp 1686, Buenos Aires, Argentina

ARTICLE INFO

Article history:
Received 3 February 2012
Returned to author for revisions
30 March 2012
Accepted 19 April 2012

Keywords:
MRCV
Fijivirus
Subcellular localization
Non-structural proteins
GFP
Confocal microscopy

ABSTRACT

The *in vivo* subcellular localization of *Mal de Río Cuarto virus* (MRCV, *Fijivirus*, *Reoviridae*) non-structural proteins fused to GFP was analyzed by confocal microscopy. P5-1 showed a cytoplasmic vesicular-like distribution that was lost upon deleting its PDZ binding TKF motif, suggesting that P5-1 interacts with cellular PDZ proteins. P5-2 located at the nucleus and its nuclear import was affected by the deletion of its basic C-termini. P7-1 and P7-2 also entered the nucleus and therefore, along with P5-2, could function as regulators of host gene expression. P6 located in the cytoplasm and in perinuclear cloud-like inclusions, was driven to P9-1 viroplasm-like structures and co-localized with P7-2, P10 and α-tubulin, suggesting its involvement in viroplasm formation and viral intracellular movement. Finally, P9-2 was *N*-glycosylated and located at the plasma membrane in association with filopodia-like protrusions containing actin, suggesting a possible role in virus cell-to-cell movement and spread.

Introduction

Mal de Río Cuarto virus (MRCV) is a member of the *Fijivirus* genus in the family *Reoviridae* that causes a severe maize disease in Argentina (Attoui et al., 2011; Lenardón et al., 1998). The virus is also able to infect several graminaceous crop species such as wheat (*Triticum aestivum*), oat (*Avena sativa*), rye (*Secale cereale*) and sorghum (*Sorghum bicolor*) (Dagoberto et al., 1985; Laguna et al., 2000; Rodriguez Pardina et al., 1998), and is transmitted in a persistent propagative manner by several species of delphacid planthoppers (Arneodo et al., 2002a; Remes Lenicov et al., 1985). The mature MRCV virion is an icosahedral double-layered particle of approximately 65 nm in diameter that has short surface spikes (A- and B-spikes) on each of the 12 vertices of the outer layer and core particle (Attoui et al., 2011). MRCV genome consists of 10 double-stranded RNA (dsRNA) segments (S1-S10). Since S5, S7 and S9 are bicistronic and the rest of the segments are monocistronic, MRCV genome putatively codes for 13 proteins (Distéfano et al., 2002, 2003, 2005; Firth and Atkins, 2009; Guzmán et al., 2007; Mongelli, 2010). MRCV replication cycle is assumed to be similar to that of other genus of the *Reoviridae* family: After viral entry to a host cell, the outer capsid is readily lost giving rise to transcriptionally active cores. New viral mRNAs are proposed to be synthesized inside the cores, egress from aqueous channels present at each of the particle vertices and translated in the cytoplasm by the cell machinery. Virus replication and assembly are known to be interdependent processes that occur in large cytoplasmic viral inclusion bodies (VIBs), named viroplasms, which are composed of viral and cellular proteins (Attoui et al., 2011). The new mature virions accumulate in cytoplasmic crystalline arrays and inside tubular structures of unknown origin. Cytopathic structures caused by *Fijivirus* infections have been thoroughly described for *Maize rough dwarf virus* (MRDV) (Gerola and Bassi, 1966; Gerola et al., 1966), *Rice black streaked dwarf virus* (RBSDV) (Isogai et al., 1998) and MRCV (Arneodo et al., 2002b). The virus cell-to-cell movement is proposed to occur through plasmodesmata in plant cells (Li et al., 2004; Wu et al., 2010) and by virus-induced tubular structures in insect cells (Wei et al., 2006). Interestingly, as it has been demonstrated for *Rotavirus* (Pesavento et al., 2006), the endoplasmic reticulum (ER) might play a role during MRCV, and possibly other fijiviruses, replication cycle (Maroniche et al., 2011). Sequence analysis of MRCV-encoded proteins, analysis of viral particle purifications and inmunogold labeling led to the identification of viral structural proteins such as a putative RNA-dependent RNA polymerase coded by S1 (P1) (Distéfano et al., 2003), a major core protein encoded by S3 (P3) (Distéfano et al., 2003, 2009), a hypothetical guanylyltransferase encoded by S4 (P4) (Distéfano et al., 2002; Supyani et al., 2007), a protein with an ATP/GTP binding motif typical of helicases encoded by S8 (P8) (Distéfano et al., 2002) and a major outer capsid protein encoded by S10 (P10) (Distéfano et al., 2005). Our preliminary results also suggest that P4 is the B-spike protein (Distéfano, 2004). Although A-spikes are

* Corresponding author. Fax: +5411 4621 0199.
E-mail address: mdelvas@cnia.inta.gov.ar (M. del Vas).

0042-6822/$ - see front matter © 2012 Elsevier Inc. All rights reserved.
http://dx.doi.org/10.1016/j.virol.2012.04.016

labile and rapidly lost upon viral particle purification (Milne et al., 1973) and thus their composition have not been unambiguously assigned to any viral protein, they were proposed to be formed by the S2 coded protein P2 (Distéfano, 2004). Segments S5, S6, S7 and S9 code for putative non-structural proteins (NSPs) P5-1, P5-2, P6, P7-1, P7-2, P9-1 and P9-2, respectively (Distéfano et al., 2003, 2005; Firth and Atkins, 2009; Guzmán et al., 2007). It has been recently demonstrated that MRCV P9-1 is the major matrix viroplasm protein and shares biochemical properties with animal reovirus counterparts (Maroniche et al., 2010). So far, the roles of the rest of MRCV NSPs remain elusive. Analyzing the subcellular distribution of viral proteins fused to fluorescent proteins or epitope-tagged has proved to be a fast and effective way to reveal their functional features (Berkova et al., 2006; Broering et al., 2005; Martin et al., 2011). Taking advantage of a novel set of Gateway-compatible vectors designed for live imaging in insect cells (Maroniche et al., 2011), we have analyzed the subcellular localization of six MRCV non-structural proteins in Sf9 insect cells and the co-localization of some of them either with each other or/and with cytoskeleton components. The results presented here shed light over their putative functions.

Results

Subcellular localization of MRCV NSPs in Sf9 cells

To define the subcellular localization of MRCV NSPs in insect cells, amino and carboxi-terminal GFP fusion proteins of P5-1, P5-2, P6, P7-1, P7-2 and P9-2 were expressed in *Spodoptera frugiperda* Sf9 cells and *in vivo* subcellular localization of all fusion proteins was analyzed by confocal microscopy.

MRCV P5-1 is a 106.9 kDa protein (Distéfano et al., 2005) that has two predicted transmembrane domains at aa 178–195 and 200–222 and a TKF motif present at its C-terminal end (Mongelli, 2010). This motif has been described as a class I PDZ-interacting domain (Harris and Lim, 2001). As shown in Fig. 1(A), GFP:P5-1 displayed an heterogeneous vesicular-like cytoplasmic distribution that did not co-localize with peroxisomes. However, P5-1:GFP was homogeneously distributed in the cytoplasm (Fig. 1(B)). Remarkably, when the putative C-terminal PDZ-interacting domain was removed, the mutant P5-1 protein fluorescent fusion (GFP:P5-1ΔTKF) distributed homogenously in the cytoplasm (Fig. 1(C)) indicating that the TKF motif may be necessary for the vesicular-like distribution of GFP:P5-1.

MRCV P5-2 is a 28.9 kDa protein with a predicted coiled-coil motif between aa 127 and 155 (Mongelli, 2010). Upon expression in Sf9 cells, GFP:P5-2 was exclusively located in the nucleus (Fig. 1(D)), whereas P5-2:GFP was found in both nucleus and cytoplasm (Fig. 1(E)). Since P5-2 has a C-terminal region rich in basic aa that might be involved in nuclear import (Kosugi et al., 2009), we constructed a truncated version of P5-2 lacking the last 36 aa, named GFP:P5-2ΔC. Such mutant's distribution was both nuclear and cytoplasmic (Fig. 1(F)), suggesting that P5-2 nuclear allocation is affected, but not impaired, by the lack of the deleted basic residues.

MRCV P6 is a 90 kDa protein (Distéfano et al., 2003) with an extensive predicted coiled-coil motif between aa 560 and 619 (Mongelli, 2010). When fluorescent fusions of P6 were expressed in Sf9 cells, GFP:P6 accumulated in one or two big cloud-like perinuclear inclusions that did not co-localize with the endoplasmic reticulum (Fig. 1(G)) or the Golgi network (Fig. 1(H)), whereas P6:GFP accumulated in the cytoplasm (Fig. 1(I)). P6 distribution was also studied by immunofluorescence using a C-terminal epitope-tagged recombinant protein (P6:V5/His). In accordance with our previous findings, P6:V5/His distributed in the cytoplasm of morphologically altered cells (i.e., irregular cytoplasm and lobulated nucleus), which were clearly different from cells expressing the cytoplasmic protein LacZ:V5 (Fig.1(J)).

MRCV P7-1 is a 41.5 kDa protein (Guzmán et al., 2007) with two predicted transmembrane domains between aa 234–251 and 286–303 (Mongelli, 2010). Both GFP:P7-1 and P7-1:GFP displayed a nucleo-cytoplasmic distribution (Fig. 2(A) and (B)). Since free GFP displays this same distribution (Fig. 2(E)), Western blot analysis on protein extracts of Sf9 cells expressing GFP:P7-1 and P7-1:GFP were performed. The expected bands for both fusion proteins were detected in the absence of free GFP (Supp. Fig. 2(A)), thus confirming that the nucleo-cytoplasmic distribution of P7-1 fusions was not due to the presence of free GFP. When further analyzing MRCV P7-1 subcellular localization by fusion to a C-terminal V5/His tag followed by immunofluorescence, the same distribution was observed (Supp. Fig. 2(B)).

MRCV P7-2 is a 36.8 kDa protein (Guzmán et al., 2007). GFP:P7-2 and P7-2:GFP were distributed into the cytoplasm (Fig. 2(C) and (D)) and in a few cases were also located in the nucleus (Fig. 2(D)). Both fluorescent fusions displayed low expression levels since only a few fluorescent cells were observed upon transfection with the corresponding plasmids.

MRCV P9-2 is a 20.5 kDa protein (Guzmán et al., 2007) with two predicted transmembrane domains at aa 49–68 and 81–105 (Mongelli, 2010). GFP:P9-2 was located at the plasma membrane (Fig. 2(F)), in association with filopodia-like protrusions that conferred an overall "hairy" phenotype to the expressing cells (Fig. 2(I)). These protrusions sometimes appeared connecting neighboring cells (Fig. 2(J)). By contrast, P9-2:GFP was not able to reach the plasma membrane and displayed partial co-localization with markers of the Golgi apparatus and the secretory pathway (Fig. 2(G) and (H)). Interestingly, P9-2 fluorescent fusions expressed in Sf9 cells and analyzed by Western blot displayed two additional bands of higher apparent molecular weights that suggested the existence of post-translational modifications (Fig. 2(K)). Because protein glycosylation can give rise to similar patterns of molecular weight shifts (Seo and Lee, 2004), we further analyzed if P9-2 fusions were glycosylated. As displayed in Fig. 2(K), PNGase treatment resulted in the loss of the lower migrating band in behalf of the intermediate migrating band which was unaltered by the treatment. Thus, our results indicate that P9-2 is *N*-glycosylated in insect cells. An additional *in silico* analysis of the MRCV P9-2 sequence by the NetNGlyc 1.0 (http://www.cbs.dtu.dk/services/NetNGlyc/) and EnsembleGly (http://turing.cs.iastate.edu/EnsembleGly/) servers detected two possible *N*-glycosylation sites at aa positions 161 and 204, the first of them being more likely to be glycosylated according to NetNGlyc.

Co-localization of MRCV NSPs with cytoskeleton components

Since there are numerous examples of virus hijacking the cytoskeleton to move within the cell (Harries et al., 2010; Lehmann et al., 2005; Leopold and Pfister, 2006), we analyzed whether MRCV NSPs co-localized with tubulin and actin and therefore which NSPs might be involved in this process. The *Spodoptera frugiperda* α-tubulin and actin genes were isolated and used to obtain fluorescent fusions that were expressed in Sf9 cells. All α-tubulin fluorescent fusions showed cytoplasmic distributions (data not shown). A partial co-localization was observed when MRCV P6 fluorescent fusions and the α-tubulin marker were co-expressed (Fig. 3(A) and (B)). Moreover, part of the tubulin was delocalized to the cytoplasmic region where GPF:P6 accumulated (Fig. 3(A)), suggesting a possible interaction between these two proteins. Since the cytoskeleton of tubulin usually provides the scaffolding for intercellular movement of viruses, we next analyzed if MRCV P6 and the α-tubulin marker were also able to co-localize with the MRCV outer capsid protein

Please cite this article as: Maroniche, G.A., et al., *In vivo* subcellular localization of *Mal de Río Cuarto virus* (MRCV) non-structural proteins in insect cells reveals their putative functions. Virology (2012), http://dx.doi.org/10.1016/j.virol.2012.04.016

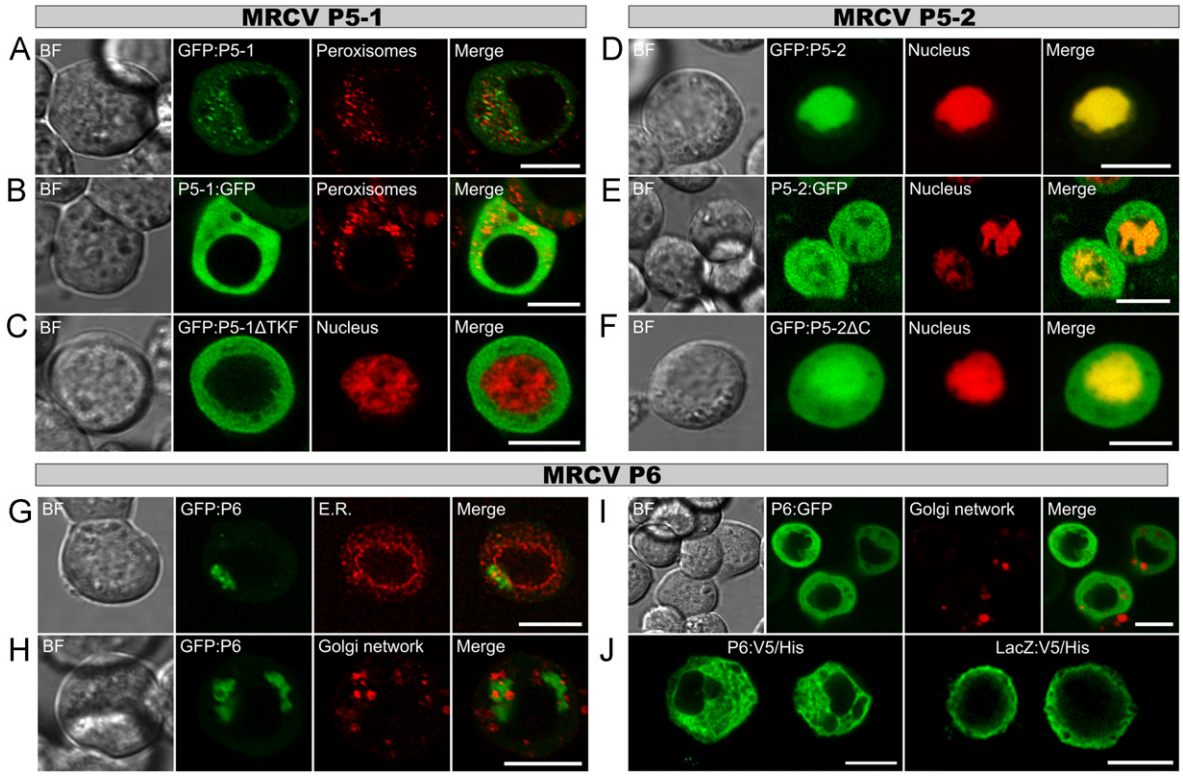

Fig. 1. Subcellular localization of MRCV P5-1, P5-2 and P6 proteins. (A)–(I) Subcellular distribution of MRCV P5-1 ((A) and (B)), P5-2 ((D) and (E)) and P6 ((G), (H) and (I)) proteins fused to GFP by either the N-terminal ((A), (D), (G) and (H)) or C-terminal end ((B), (E) and (I)), transiently expressed in Sf9 cells and examined by live fluorescent imaging. Mutant versions of MRCV P5-1 (C) and P5-2 (F) were also analyzed. Peroxisomes, nucleus, ER and Golgi network organelles were visualized by mCherry-based fluorescent markers that were previously developed and validated (Maroniche et al., 2011). In each case, images of the bright field (BF), MRCV fluorescent fusion, fluorescent organelle marker and the merge of the fluorescence are shown. (J) Subcellular distribution of V5-tagged MRCV P6 and ß-galactosidase control protein transiently expressed in Sf9 cells and examined by direct immunofluorescence. Scale bars = 10 μm.

P10. It was observed that, when co-expressed, the three proteins completely co-localized in a big and irregular perinuclear structure (Fig. 3(C)). This same subcellular distribution was detected by co-localization of MRCV P10 with α-tubulin in the absence of MRCV P6 (Pearson coefficient = 0.93) (Fig. 3(D)) and by co-localization of MRCV P10 and P6 (Pearson coefficient = 0.96) (Fig. 3(E)). Taken together, these results suggest that MRCV P6 and P10 might be able to associate with each other and/or with the cellular microtubules.

On the other hand, it is well established that extending actin bundles are an important component of animal cells filopodia (Mattila and Lappalainen, 2008). Accordingly, we noticed that the filopodia-like structures observed in GFP:P9-2 expressing cells partially co-localized with the actin marker (Fig. 3(F)). This result indicates that the filopodia-like structures where MRCV P9-2 is located are actin-based, establishing a possible association of P9-2 with the actin cytoskeleton.

Co-localization of MRCV NSPs

Our group has recently shown that MRCV P9-1 is the major matrix viroplasm protein (Maroniche et al., 2010). Since viroplasms are usually composed of other viral and cellular proteins, we carried out a series of co-localization analysis to identify other putative viroplasm components. In the presence of MRCV P9-1 with a free C-terminal end, MRCV P6 was driven to the VIB-like bodies formed by MRCV P9-1 (Fig. 4(A)). However, when the C-terminal end of MRCV P9-1 was blocked by the fluorescent fusion, MRCV P6 remained free in the cytoplasm (Fig. 4(B)). In addition, MRCV P6 was as well able to co-localize with MRCV P7-2 (Fig. 4(C)). Altogether, our results suggest that MRCV P6 may be part of functional viroplasms during infection and that it might recruit MRCV P7-2 to these structures.

Discussion

The functional roles of *Fijivirus* NSPs have been relatively poorly studied when compared to *Phytoreovirus* such as *Rice dwarf virus* (RDV) and *Rice gall dwarf virus* (RGDV) NSPs. This is partially due to the lack of planthopper tissue-culture cell lines permissive to *fijivirus* infection. In this context, transient expression of fluorescent proteins in non-host insect cells stands as a suitable means to study *Fijivirus* protein functions. Our group has recently developed a novel set of Gateway-compatible vectors for live imaging in lepidopteran insect cells (Maroniche et al., 2011). To shed light on the putative functions of MRCV NSPs, we have analyzed their subcellular distribution in Sf9 cells and determined whether there was co-localization, either with each other or/and with cytoskeleton components. It has been stressed out that when fluorescent fusions are used to study the subcellular localization of a protein for which only minimal information is available, it is important to analyze both N and C-terminal fusion proteins to maximize the likelihood of giving rise to functional and properly targeted quimeric proteins (Müller-Taubenberger, 2006). Consequently, we decided to construct fluorescent fusions of MRCV NSPs by placing GFP on either the N or C-termini. This strategy proved to be appropriate and led us to detect possible interaction or targeting domains in the termini of some of the studied MRCV proteins (see below).

Virus infection causes profound changes in the expression of host genes. For example, thousands of genes are differentially

Please cite this article as: Maroniche, G.A., et al., *In vivo* subcellular localization of *Mal de Río Cuarto virus* (MRCV) non-structural proteins in insect cells reveals their putative functions. Virology (2012), http://dx.doi.org/10.1016/j.virol.2012.04.016

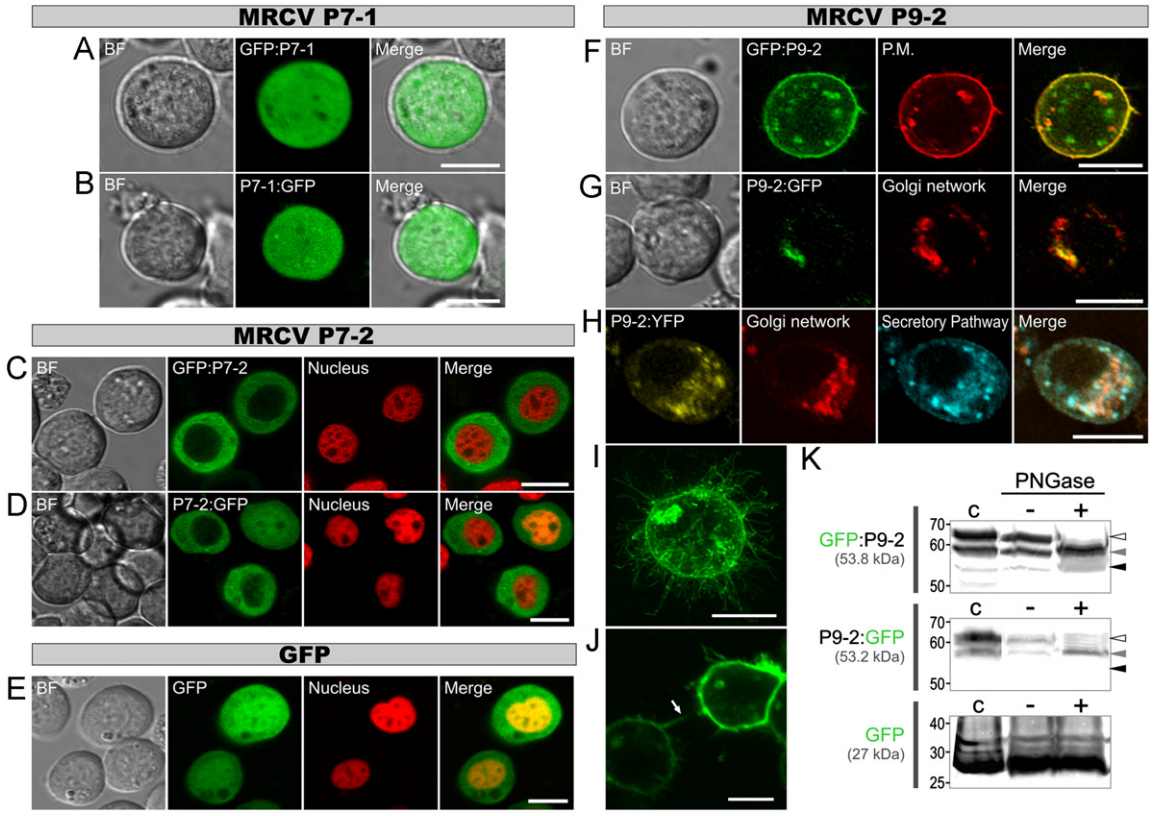

Fig. 2. Subcellular localization of MRCV P7-1, P7-2 and P9-2 proteins. ((A)–(D) and (F)–(J)) Subcellular distribution of MRCV P7-1 ((A) and (B)), P7-2 ((C) and (D)) and P9-2 ((F)–(J)) proteins fused to GFP or YFP by either the N-terminal ((A), (C), (F), (I) and (J)) or C-terminal ends ((B), (D), (G) and (H)), transiently expressed in Sf9 cells and examined by live fluorescent imaging. In addition, free GFP protein was expressed as a control (K). Nucleus, plasma membrane (P.M.), Golgi network and secretory pathway organelles were visualized using fluorescent markers previously developed and validated (Maroniche et al., 2011) (see Materials and methods section). Images of the bright field (BF), MRCV fluorescent fusion, fluorescent organelle marker and/or the merge of the fluorescence are shown as indicated in the figure. (H) Partial co-localization of P9-2:YFP with Golgi network and secretory pathway organelle markers constructed by fusion to mCherry and CFP fluorescent proteins, respectively. ((I) and (J)) Sf9 cells expressing GFP:P9-2 showing the overall phenotype by fluorescence maximum projection (I) and filopodia-like protrusions connecting adjacent cells indicated with an arrow (J). Scale bars = 10 μm. (K) Glycosylation analysis of MRCV P9-2 expressed in Sf9 cells. MRCV P9-2 fluorescent fusions in total protein cell extracts that were non-treated (C), or treated with (+) or without (−) PNGase, were detected by Western blot using an anti-GFP antibody. Cells expressing GFP were used as a negative control. The three proteins analyzed and their expected molecular weights are depicted to the left of the figure. Numbers on the side of the blot indicate protein molecular weight markers (kDa). Black arrows indicate the bands of an apparent molecular weight expected for the MRCV P9-2 fusions, while gray and white arrows indicate two additional bands of higher apparent molecular weights.

expressed upon plant reovirus infection (Jia et al., 2011; Li et al., 2011; Satoh et al., 2011; Supyani et al., 2007). These changes could be caused by a direct effect of specific viral proteins entering the nucleus and participating in the transcriptional regulation of host genes. RBSDV minor core protein P8 is the only *Fijivirus* protein that has been so far described as able to enter the nucleus and repress transcription (Liu et al., 2007). In this work, we have observed that three MRCV NSPs (P5-2, P7-1 and P7-2) located at the cell nucleus of S9 cells, even when lacking detectable nuclear localization sequences (Mongelli, 2010). MRCV P5-2 entered and remained exclusively in the nucleus when expressed as an N-terminal GFP fusion. Nuclear localization was affected when GFP blocked the C-terminal end and also when 36 aa of the C-terminal end were deleted, suggesting that the C-terminal tail, rich in basic residues, is in part responsible for the protein nuclear localization. Secondly, MRCV P7-1 showed a nucleo-cytoplasmic localization when fused to GFP or to a V5 C-terminal epitope. Since MRCV P7-1 fusion to GFP resulted in a 71.2 kDa protein (a size that exceeds the size-exclusion limit of the nuclear pore complexes) (Hoelz et al., 2011), it might be actively transported to the cell nucleus. Finally, MRCV P7-2 distribution was predominately cytoplasmic, but in some cases it was able to enter the nucleus. Although the reason for this dual localization is unknown, it is interesting to note that MRCV P7-2 is able to act as a strong transcriptional activator in a Yeast Two Hybrid system (Llauger et al., unpublished results). Therefore, MRCV P5-2, P7-1 and P7-2 nuclear localization might underlie a role in direct or indirect transcriptional regulation of host genes. It is interesting to point out that most transcription factors bind DNA in a dimeric state and MRCV P5-2 has a predicted coiled-coil motif between aa positions 127 and 155 (Mongelli, 2010) that could mediate dimerization.

Reovirus genome replication and the first steps of virus morphogenesis take place in VIBs or viroplasms which are highly dynamic structures that are readily formed after viral entry to the host cell (Attoui et al., 2011). We have recently proposed that MRCV P9-1 is the viroplasm matrix protein on account of its ability to self-associate giving rise to viral inclusion bodies resembling viroplasms when expressed in insect cells and, in addition, it shares other biochemical properties with animal reoviruses viroplasm proteins (Maroniche et al., 2010). However, the rest of MRCV viroplasm components remained to be identified. MRCV P6 is the most variable MRCV-encoded protein showing a 44.8% identity with its closest counterpart RBSDV P6 (Distéfano et al., 2003). This relatively low identity is mainly due to a highly variable coiled-coil domain located between aa residues 560 and 619. MRCV P6 fusion to GFP or to a V5 epitope by its C-terminal end resulted in a cytoplasmic distribution. By contrast, when its C-terminal end was free, MRCV P6 accumulated in one or two big cloud-like perinuclear structures. Importantly,

Please cite this article as: Maroniche, G.A., et al., *In vivo* subcellular localization of *Mal de Río Cuarto virus* (MRCV) non-structural proteins in insect cells reveals their putative functions. Virology (2012), http://dx.doi.org/10.1016/j.virol.2012.04.016

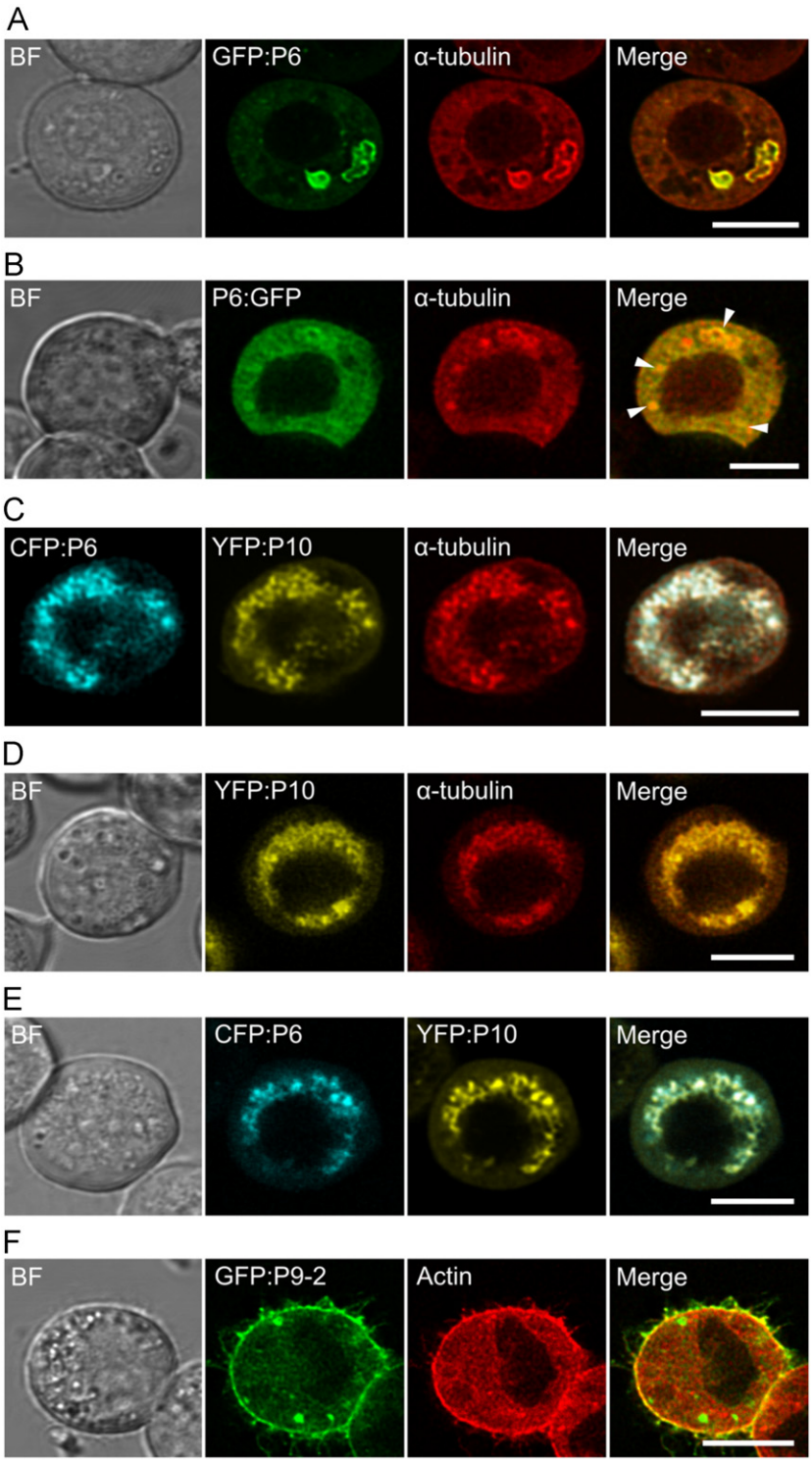

Fig. 3. Co-localization of MRCV proteins with cellular cytoskeleton components. ((A) and (B)) Partial co-localization of MRCV P6 fluorescent fusions with a α-tubulin fluorescent marker. White arrows indicate areas of co-localization. (C–E) Co-localization of MRCV P6, P10 and α-tubulin when co-expressed (C) or expressed in pairs ((D) and (E)). (F) Partial co-localization of GFP:P9-2 with an actin fluorescent marker in filopodia-like protrusions present in the plasma membrane of Sf9 cells. The α-tubulin and actin cytoskeletal proteins were visualized as fusions to mCherry (see Materials and methods). In each case, images of the bright field (BF), MRCV fluorescent fusion, mCherry-based fluorescent marker and the merge of the fluorescence are shown as indicated in the figure. Scale bars = 10 μm.

the fact that MRCV P6 was recruited to the VIB-like cytoplasmic structures formed by MRCV P9-1 suggests that this protein is playing a role at the viroplasms. Recent studies have demonstrated that RBSDV P6 gives rise to viroplasm-like inclusions in plant cells and that it is able to recruit the viroplasm associated protein RBSDV P9-1 to these structures (Wang et al., 2011). These somehow conflicting results may reflect differences in the mechanisms involved in the process of viroplasm nucleation in plant and insect *Fijivirus* hosts, but further work will be necessary to support this hypothesis. In addition, MRCV P6 was also able to delocalize MRCV P7-2 and to completely co-localize with MRCV P10, supporting the hypothesis that MRCV P6 might be able to

Please cite this article as: Maroniche, G.A., et al., *In vivo* subcellular localization of *Mal de Río Cuarto virus* (MRCV) non-structural proteins in insect cells reveals their putative functions. Virology (2012), http://dx.doi.org/10.1016/j.virol.2012.04.016

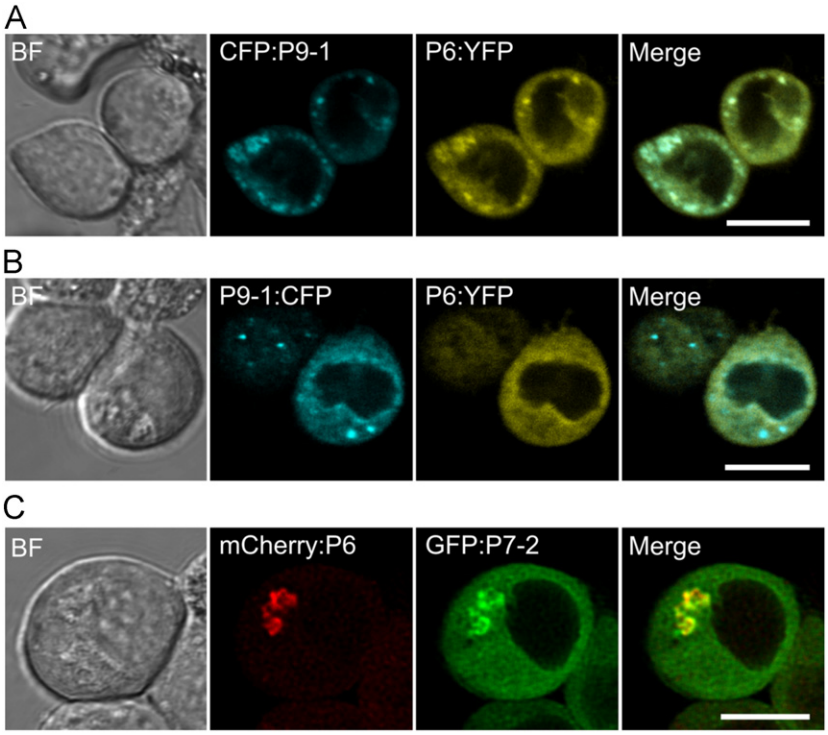

Fig. 4. Co-localization of MRCV NSPs. ((A) and (B)) Co-expression of MRCV P6 and MRCV P9-1 fluorescent fusions showing partial co-localization (A) or no co-localization (B) depending if P9-1 C-terminal end is free or blocked. (C) Partial co-localization of MRCV P6 and P7-2 fluorescent fusions in cytoplasmic cloud-like aggregates. In all cases, images of the bright field (BF), MRCV fluorescent fusions and the merge of the fluorescence are shown as indicated in the figure. Scale bars = 10 μm.

recruit viral (and possibly cellular proteins) to the viroplasms. A similar role has recently been demonstrated for *Rotavirus* NSP5 and *Orthoreovirus* μNS non-structural major viroplasm proteins (Contin et al., 2010; Miller et al., 2010).

When analyzing MRCV P5-1 *in vivo* subcellular localization, we observed that GFP:P5-1 was distributed in vesicle-like structures and that did not co-localize with a peroxisomal marker. Moreover, we proved this distribution to be dependent on a MRCV P5-1 C-terminal TKF motif. Since this signal is a putative type I PDZ domain-binding motif (PBM) (Harris et al., 2001), it is possible that the distribution pattern of P5-1 is due to an interaction with cellular PDZ proteins. Indeed, several animal pathogenic viruses encode PBMs that mediate interactions with a select group of cellular PDZ proteins involved in intracellular signaling and cellular polarization processes (Brone and Eggermont, 2005). Furthermore they were found to be required to enhance viral replication and dissemination in the host (Javier and Rice, 2011). For the insect vector to become infective, plant reoviruses must first replicate in epithelial cells of the alimentary canal, then spread to the rest of the body and finally reach the salivary glands. For example, the phytoreovirus RDV accumulates first in the leafhopper's filter chamber and anterior midgut epithelia and subsequently spreads to the nervous system and other tissues (Chen et al., 2011). The regulation of viral intracellular transport in polarized cells, such as midgut epithelial cells, might be thus vital for MRCV infection. Further work is necessary to find out if MRCV P5-1 is able to interact with PDZ proteins and, if so, the biological meaning of such interactions in MRCV replication cycle should also be analyzed. MRCV S5 putatively codes for two proteins since it contains a big 5′ ORF that codes for MRCV P5-1 (Distéfano et al., 2005) and an initially unnoticed overlapping 3′ ORF that codes for MRCV P5-2 (Firth and Atkins, 2009). The second ORF could be expressed by several mechanisms including shunting, reinitiation or IRES activity (Firth and Atkins, 2009). Alternatively, ORF 5-2 could be translated by a +1 frameshifting from ORF5-1. If this was the case, the fusion P5-1/P5-2 product would be devoid of the putative PBM and therefore have a different localization and function than MRCV P5-1.

Fijivirus intra-cellular movement during infection of both plant and insect hosts has received little attention. Pioneering excellent electron microscopy work has established that, during *Fijivirus* replication cycle, the newly assembled mature virions locate at the surroundings of viroplams, from where they are assumed to move towards the cell periphery (Favali et al., 1974). Our work showed that the MRCV major outer capsid protein P10 co-localizes with tubulin and MRCV P6. This not only indicates that the microtubule network may participate in MRCV intracellular movement as has been demonstrated for RGDV (*Phytoreovirus, Reoviridae*) (Wei et al., 2009), but also suggests that MRCV P6 might intervene in the movement of mature virus particles from the viroplams to the cell periphery.

Tubular inclusions formed during plant reovirus replication have long been detected in ultrathin sections of infected plant and insect cells by electron microscopy (Conti and Lovisolo, 1971; Fukushi et al., 1962; Giannotti and Milne, 1977; Shikata and Kitagawa, 1977). For members of the *Phytoreovirus* genus, the use of cultured insect vector cells has allowed the study of the viral spread showing that RDV intercellular movement is dependent on the virus-induced tubular structures composed of Pns10 that move along actin-based filopodia into adjacent cells (Wei et al., 2006). By contrast, very little is known on *Fijivirus* spread. In RBSDV-infected insect and plant cells, tubular structures were shown to react with antibodies raised against RBSDV P7-1 (Isogai et al., 1998). In accordance with this, the homologous SRBSDV P7-1 fused to an 8 aa tag in its C-terminus is able to self-interact and form tubular structures when expressed from a recombinant baculovirus in Sf9 cells (Liu et al., 2011). Somehow surprisingly, we did not observe MRCV P7-1 clearly forming this kind of

Please cite this article as: Maroniche, G.A., et al., *In vivo* subcellular localization of *Mal de Río Cuarto virus* (MRCV) non-structural proteins in insect cells reveals their putative functions. Virology (2012), http://dx.doi.org/10.1016/j.virol.2012.04.016

structures in Sf9 cells when fused to a C-terminus short epitope or to GFP, even when tubules have been found in MRCV-infected wheat (but interestingly not in maize) cells (Arneodo et al., 2002b). While the different properties reported for P7-1 may reflect real differences between MRCV and RBSDV (both P7-1 proteins are 61.3% identical), they might also be a consequence of the expression systems used in each case (transfection with a MRCV P7-1 expression plasmid vs. SRBSDV P7-1 expressed by a recombinant baculovirus).

Finally, our results revealed that MRCV P9-2 is located at the plasma membrane of Sf9 cells, a distribution that required a free C-terminal end. Since a GFP fusion to the N-terminal end of MRCV P9-2 did not interfere with its targeting to the secretion pathway, its trafficking might not involve the canonical mechanism that requires an N-terminal signal peptide (Zimmermann et al., 2011). We next demonstrated that MRCV P9-2 is *N*-glycosylated and that it may undergo a second post-translational modification yet to be identified. Overall, the features of MRCV P9-2 (178 aa) described here resemble those of *Orbivirus* NS3 and *Rotavirus* NSP4, which are both relatively small (229 and 175 aa, respectively) non-structural integral membrane glycoproteins that play important roles in virus entry, morphogenesis and release (Estes and Kapikian, 2007; Roy and Noad, 2006). These resemblances support a possible role of MRCV P9-2 in viral transport across plasma membrane and/or morphogenesis. Interestingly, MRCV P9-2 was observed in association with superficial filopodia-like formations that contained actin and sometimes connected neighboring cells. Extending actin bundles are an important component of filopodia in animal cells (Mattila and Lappalainen, 2008) and various viruses undergo rapid actin- and myosin-driven transport to cell entry sites (Lehmann et al., 2005). Whether MRCV P9-2 is able to bind actin filaments and whether this association is important for P9-2 proposed role in viral movement and spread are open questions that remain to be addressed.

This study represents the first step towards understanding the role of MRCV non-structural proteins throughout the viral replication cycle. Future efforts on a more profound characterization of each MRCV protein will improve our understanding of the pathosystem. In addition, since it has been shown that silencing of several plant reovirus genes with different roles during viral infection in transgenic host plants is not equally effective in conferring tolerance to the related disease (Shimizu et al., 2011), our results might have practical consequences in the development of effective antiviral RNAi strategies.

Materials and methods

Plasmid construction

Based on a collection of pCR8/GW/TOPO (Invitrogen, USA) entry vectors containing MRCV NSPs coding sequences with or without their initiation or stop codon (Mongelli, 2010) and a set of Gateway destination vectors for live imaging in insect cells that we have recently developed (Maroniche et al., 2011), amino and carboxi-terminal GFP fusion proteins were obtained for all MRCV NSPs using the LR Clonase II enzyme mix (Invitrogen, USA) according to the manufacturer's protocol. Similarly, V5/His-tagged versions of MRCV P6 and P7-1 were constructed by recombination of the proper entry vectors and the pIB/V5-His-DEST destination vector (Invitrogen, USA). All MRCV expression vectors used in this work are schematized in Supplementary Fig. 1. As controls, free GFP was expressed using a pIB-V5/His derivative that contains the GFP coding region from pEGFP-1 (Clontech, Japan) and V5/His-tagged β-glucuronidase was expressed using pIB/V5-His-GW/lacZ plasmid (Invitrogen, USA).

Cell organelles were tracked using a collection of fluorescent markers that were developed and validated in a previous work (Maroniche et al., 2011). mCherry-based fluorescent fusions were used for nucleus, Golgi network, peroxisomes, plasma membrane, ER and actin, while a CFP fusion was used for the secretion pathway marker. To construct a tubulin fluorescent marker, the *S. frugiperda* α-tubulin gene was isolated by RT-PCR from Sf9 total RNA using primers Sf9aTub Forw s/atg (CGTGAGTGCATCTCAG-TAC) and Sf9aTub Rev (TTAGTATTCCTCTGCTCC), cloned into pCR8/GW/TOPO (Invitrogen, USA) and automatically sequenced (GenBank accession: HQ008728). The resulting plasmid was used for recombination with pIB-RW (Maroniche et al., 2011) to obtain a N-terminal fluorescent fusion to mCherry.

Cell culture and transfection

Spodoptera frugiperda Sf9 (IPLBSF21-AE clonal isolate 9) cells were seeded into 35 mm Glass Bottom Culture Dishes (MatTek Corporation, Ashland, MA, USA) using Sf900II Serum free media medium (Invitrogen, USA) supplemented with 2% fetal bovine serum (Invitrogen, USA), and incubated at 27 °C until 60–70% confluence. Cells were then transfected with 1 μg of each plasmid using Cellfectin II transfection reagent (Invitrogen, USA) according to the manufacturer's instructions, and incubated at 27 °C until used.

Fluorescence live imaging

At 48–72 h post-transfection, the culture medium was replaced with phosphate buffered saline pH 6.2 and transfected cells were used for fluorescence imaging in a Leica TCS-SP5 (Leica Microsystems GmbH, Wetzlar, Germany) spectral laser confocal microscope using a 63x objective (HCX PL APO CS 63.0 × 1.20 WATER UV). The 458, 488 and 514 nm lines of the Argon laser were used for CFP, GFP and YFP excitation, respectively, and the 543 nm line from the HeNe laser was employed for mCherry excitation. Scanning was performed in sequential mode to minimize signal bleed-through, and fluorescence emission was detected with the following channel settings: 465–505 nm for CFP, 498–540 nm for GFP, 525–600 nm for YFP and 610– 670 nm for mCherry. The microscope power settings, detectors gain and scanning speed were adjusted to optimize contrast and resolution for each individual image. The images collected in stacks were 3D-deconvoluted using the AutoQuant X2 software (Media Cybernetics Inc., USA). Co-localizations were analyzed by calculating the Pearson's correlation coefficient with the co-localization module of the Leica LAS AF software.

Protein analysis and Immunodetection

Total proteins of Sf9 cells grown in each well of a 6-well plate were extracted using 50 μl of cell lysis buffer (50 mM Tris [pH 7.5], 150 mM NaCl, 1% NP40, 0.1% Triton N-X100). The resulting lysates were centrifuged 5 min at maximum speed in a refrigerated microcentrifuge to pellet the nuclei and cell debris, and the supernatant containing the protein samples were subjected to SDS-PAGE and subsequent Western blot experiments. To detect the fluorescent fusions or the V5-tagged proteins, a rabbit anti-GFP polyclonal antibody and a mouse anti-V5 monoclonal antibody were used, respectively, according to the manufacturer's protocol (Invitrogen, USA). Protein immunofluorescence assays were carried out using a mouse anti-V5 monoclonal antibody conjugated to FITC (Maroniche et al., 2010).

The MRCV P9-2 glycosylation assay was performed using Peptide *N*-Glycosidase F (PNGase F, NEB, Germany), according to the manufacturers protocol.

Please cite this article as: Maroniche, G.A., et al., *In vivo* subcellular localization of *Mal de Río Cuarto virus* (MRCV) non-structural proteins in insect cells reveals their putative functions. Virology (2012), http://dx.doi.org/10.1016/j.virol.2012.04.016

Acknowledgments

GAM, VCM and GL hold a doctoral fellowship from the Consejo Nacional de Investigaciones Científicas y Técnicas (CONICET). VA, OT and MdV are career members of CONICET. The authors would like to thank Dr. Sebastián Asurmendi, Dr. Natalia Almasia, Dr. Julia Sabio y García and Dr. Esteban Hopp for the critical reading of the manuscript and Dr. Julia Sabio y García and Dr. Eleonora Campos for excellent English language editing.

Appendix A. Supporting information

Supplementary data associated with this article can be found in the online version at http://dx.doi.org/10.1016/j.virol.2012.04.016.

References

Arneodo, J.D., Guzmán, F.A., Conci, L.R., Laguna, I.G., Truol, G.A., 2002a. Transmission features of *Mal de Río Cuarto virus* in wheat by its planthopper vector *Delphacodes kuscheli*. Ann.Appl. Biol. 141, 195–200.

Arneodo, J.D., Lorenzo, E., Laguna, I.G., Abdala, G., Truol, G.A., 2002b. Cytopathological characterization of *Mal de Río Cuarto virus* in corn, wheat and barley. Fitopatol. Bras. 27, 298–302.

Attoui, H., Mertens, P.P.C., Becnel, J., Belaganahalli, S., Bergoin, M., Brussaard, C.P., Chappell, J.D., Ciarlet, M., del Vas, M., Dermody, T.S., Dormitzer, P.R., Duncan, R., Fang, Q., Graham, R., Guglielmi, K.M., Harding, R.M., Hillman, B., Makkay, A., Marzachì, C., Matthijnssens, J., Milne, R.G., Mohd Jaafar, F., Mori, H., Noordeloos, A.A., Omura, T., Patton, J.T., Rao, S., Maan, M., Stoltz, D., Suzuki, N., Upadhyaya, N.M., Wei, C., Zhou, H., 2011. Family reoviridae. In: King, A.M.Q., Adams, M.J., Castens, E.B., Lefkowitz, E.J. (Eds.), Virus Taxonomy: Ninth Report of the International Comittee on Taxonomy of Viruses. Elsevier, San Diego, pp. 541–638.

Berkova, Z., Crawford, S.E., Trugnan, G., Yoshimori, T., Morris, A.P., Estes, M.K., 2006. Rotavirus NSP4 induces a novel vesicular compartment regulated by calcium and associated with viroplasms. J Virol. 80, 6061–6071.

Broering, T.J., Arnold, M.M., Miller, C.L., Hurt, J.A., Joyce, P.L., Nibert, M.L., 2005. Carboxyl-proximal regions of reovirus nonstructural protein muNS necessary and sufficient for forming factory-like inclusions. J. Virol. 79, 6194–6206.

Brone, B., Eggermont, J., 2005. PDZ proteins retain and regulate membrane transporters in polarized epithelial cell membranes. Am. J Physiol 288, C20–29.

Conti, M., Lovisolo, O., 1971. Tubular structures associated with maize rough dwarf virus particles in crude extracts: electron microscopy study. J Gen. Virol. 13, 173–176.

Contin, R., Arnoldi, F., Campagna, M., Burrone, O.R., 2010. Rotavirus NSP5 orchestrates recruitment of viroplasmic proteins. J. Gen. Virol. 91, 1782–1793.

Chen, H., Chen, Q., Omura, T., Uehara-Ichiki, T., Wei, T., 2011. Sequential infection of rice dwarf virus in the internal organs of its insect vector after ingestion of virus. Virus Res. 160, 389–394.

Dagoberto, E., Remes Lenicov, A.M.d., Tesón, A., Paradell, S., 1985. Avena sativa L. hospedante preferencial del transmisor del "*Mal de Río Cuarto*" Delphacodes kuscheli Fennah. (Homoptera-Delphacidae). Neotropical 31, 82.

Distéfano, A.J., 2004. Caracterización molecular del *Mal de Río Cuarto virus* (MRCV) del maíz: estudio de los segmentos genómicos S1-S6, S8 y S10 y de las proteínas codificadas por los mismos., Facultad de Ciencias Exactas y Naturales (FCEyN). Universidad de Buenos Aires.

Distéfano, A.J., Conci, L.R., Muñoz Hidalgo, M., Guzmán, F.A., Hopp, H.E., del Vas, M., 2002. Sequence analysis of genome segments S4 and S8 of *Mal de Rio Cuarto virus* (MRCV): evidence that the virus should be a separate *Fijivirus* species. Arch. Virol. 147, 1699–1709.

Distéfano, A.J., Conci, L.R., Muñoz Hidalgo, M., Guzmán, F.A., Hopp, H.E., del Vas, M., 2003. Sequence and phylogenetic analysis of genome segments S1, S2, S3 and S6 of *Mal de Rio Cuarto virus*, a newly accepted *Fijivirus* species. Virus Res. 92, 113–121.

Distéfano, A.J., Hopp, H.E., del Vas, M., 2005. Sequence analysis of genome segments S5 and S10 of *Mal de Rio Cuarto virus* (*Fijivirus*, Reoviridae). Arch. Virol. 150, 1241–1248.

Distéfano, A.J., Maldonado, S., Hopp, H.E., del Vas, M., 2009. *Mal de Rio Cuarto virus* (MRCV) genomic segment S3 codes for the major core capsid protein. Virus Genes 38, 455–460.

Estes, M.K., Kapikian, A.Z., 2007. Rotaviruses. In: Knipe, D.M.a.H, P.E. (Eds.), Fields Virology, 5th edn. Wolters Kluwer-Lippincott Williams and Wilkins, Philadelphia, pp. 1917–1974.

Favali, M.A., Bassi, M., Appiano, A., 1974. Synthesis and migration of maize rough dwarf virus in the host Cell: an autoradiographic study. J. Gen. Virol. 24, 563–565.

Firth, A.E., Atkins, J.F., 2009. Analysis of the coding potential of the partially overlapping 3′ ORF in segment 5 of the plant fijiviruses. Virol. J. 6, 32.

Fukushi, T., Shikata, E., Kimura, I., 1962. Some morphological characters of rice dwarf virus. Virology 18, 192–205.

Gerola, F.M., Bassi, M., 1966. An electron microscopy study of leaf vein tumours from maize plants experimentally infected with maize rough dwarf virus. Caryologia 19, 13.

Gerola, F.M., Bassi, M., Lovisolo, O., Vidano, C., 1966. Virus-like particles in both maize plants infected with maize rough dwarf virus and the vector Laodelphax striatellus Fallén. Phytopathol. Zeits. 56, 97–99.

Giannotti, J., Milne, R.G., 1977. Pangola stunt virus in thin sections and in negative stain. Virology 80, 347–355.

Guzmán, F.A., Distéfano, A.J., Arneodo, J.D., Hopp, H.E., Lenardon, S.L., del Vas, M., Conci, L.R., 2007. Sequencing of the bicistronic genome segments S7 and S9 of *Mal de Rio Cuarto virus* (*Fijivirus*, Reoviridae) completes the genome of this virus. Arch. Virol. 152, 565–573.

Harries, P.A., Schoelz, J.E., Nelson, R.S., 2010. Intracellular transport of viruses and their components: utilizing the cytoskeleton and membrane highways. Mol. Plant Microbe Interact. 23, 1381–1393.

Harris, B.Z., Lim, W.A., 2001. Mechanism and role of PDZ domains in signaling complex assembly. J. Cell Sci. 114, 3219–3231.

Harris, M.J., Kuwano, M., Webb, M., Board, P.G., 2001. Identification of the apical membrane-targeting signal of the multidrug resistance-associated protein 2 (MRP2/MOAT). J. Biol. Chem. 276, 20876–20881.

Hoelz, A., Debler, E.W., Blobel, G., 2011. The structure of the nuclear pore complex. Annu. Rev. Biochem. 80, 613–643.

Isogai, M., Uyeda, I., Lee, B.C., 1998. Detection and assignment of proteins encoded by rice black streaked dwarf fijivirus S7, S8, S9 and S10. J. Gen. Virol. 79 (Pt 6), 1487–1494.

Javier, R.T., Rice, A.P., 2011. Emerging theme: cellular PDZ proteins as common targets of pathogenic viruses. J. Virol.

Jia, M.A., Li, Y., Lei, L., Di, D., Miao, H., Fan, Z., 2011. Alteration of gene expression profile in maize infected with a double-stranded RNA *Fijivirus* associated with symptom development. Mol. Plant Pathol.

Kosugi, S., Hasebe, M., Matsumura, N., Takashima, H., Miyamoto-Sato, E., Tomita, M., Yanagawa, H., 2009. Six classes of nuclear localization signals specific to different binding grooves of importin alpha. J. Biol. Chem. 284, 478–485.

Laguna, I.G., Giménez Pecci, M.P., Herrera, P.S., Borgogno, C., Ornaghi, J.A., Rodriguez Pardina, P., 2000. Rol de los cereales en la epidemiología del virus del Mal de Río Cuarto en Argentina. Fitopatol. Bras. 35, 41–49.

Lehmann, M.J., Sherer, N.M., Marks, C.B., Pypaert, M., Mothes, W., 2005. Actin- and myosin-driven movement of viruses along filopodia precedes their entry into cells. J. Cell Biol. 170, 317–325.

Lenardón, S.L., March, G.J., Nome, S.F., Ornaghi, J.A., 1998. Recent outbreak of *Mal de Río Cuarto virus* on corn in Argentina. Plant Dis. 82, 448.

Leopold, P.L., Pfister, K.K., 2006. Viral strategies for intracellular trafficking: motors and microtubules. Traffic (Copenhagen, Denmark) 7, 516–523.

Li, K., Xu, C., Zhang, J., 2011. Proteome profile of maize (Zea Mays L.) leaf tissue at the flowering stage after long-term adjustment to rice black-streaked dwarf virus infection. Gene 485, 106–113.

Li, Y., Bao, Y.M., Wei, C.H., Kang, Z.S., Zhong, Y.W., Mao, P., Wu, G., Chen, Z.L., Schiemann, J., Nelson, R.S., 2004. Rice dwarf phytoreovirus segment S6-encoded nonstructural protein has a cell-to-cell movement function. J. Virol. 78, 5382–5389.

Liu, H., Wei, C., Zhong, Y., Li, Y., 2007. Rice black-streaked dwarf virus minor core protein P8 is a nuclear dimeric protein and represses transcription in tobacco protoplasts. FEBS Lett. 581, 2534–2540.

Liu, Y., Jia, D., Chen, H., Chen, Q., Xie, L., Wu, Z., Wei, T., 2011. The P7-1 protein of southern rice black-streaked dwarf virus, a *fijivirus*, induces the formation of tubular structures in insect cells. Arch.Virol.

Maroniche, G.A., Mongelli, V.C., Alfonso, V., Llauger, G., Taboga, O., del Vas, M., 2011. Development of a novel set of gateway-compatible vectors for live imaging in insect cells. Insect Mol. Biol. 20, 675–685.

Maroniche, G.A., Mongelli, V.C., Peralta, A.V., Distéfano, A.J., Llauger, G., Taboga, O.A., Hopp, E.H., del Vas, M., 2010. Functional and biochemical properties of *Mal de Rio Cuarto virus* (*Fijivirus*, Reoviridae) P9-1 viroplasm protein show further similarities to animal reovirus counterparts. Virus Res. 152, 96–103.

Martin, K.M., Dietzgen, R.G., Wang, R., Goodin, M.M., 2011. Lettuce necrotic yellows cytorhabdovirus protein localization and interaction map and comparison with nucleorhabdoviruses. J. Gen. Virol.

Mattila, P.K., Lappalainen, P., 2008. Filopodia: molecular architecture and cellular functions. Nat. Rev. 9, 446–454.

Milne, R.G., Conti, M., Lisa, V., 1973. Partial purification, structure and infectivity of complete maize rough dwarf virus particles. Virology 53, 130–141.

Miller, C.L., Arnold, M.M., Broering, T.J., Hastings, C.E., Nibert, M.L., 2010. Localization of mammalian orthoreovirus proteins to cytoplasmic factory-like structures via nonoverlapping regions of microNS. J Virol. 84, 867–882.

Mongelli, V.C., 2010. Estudio funcional de las proteínas codificadas por el virus del *Mal de Río Cuarto* en hospedantes vegetales., facultad de Ciencias Exactas y Naturales. Universidad de Buenos Aires, Buenos Aires, Argentina, p. 136.

Müller-Taubenberger, A., 2006. Application of Fluorescent Protein Tags as Reporters in Live-Cell Imaging Studies. Springer, Totowa, NJ.

Pesavento, J.B., Crawford, S.E., Estes, M.K., Prasad, B.V., 2006. Rotavirus proteins: structure and assembly. Curr. Top. Microbiol. Immunol. 309, 189–219.

Remes Lenicov, A.M.d., Teson, A., Dagoberto, E., Huguet, N., 1985. Hallazgo de uno de los vectores del *Mal de Río Cuarto* en maíz. Gac. Agropecuaria 25, 251–258.

Rodriguez Pardina, P., Giménez Pecci, M.P., Laguna, I.G., 1998. Wheat: a new natural host for the *Mal de Río Cuarto Virus* in the endemic disease area, Río Cuarto, Córdoba province, Argentina. Plant Dis. 82, 149–152.

Please cite this article as: Maroniche, G.A., et al., *In vivo* subcellular localization of *Mal de Río Cuarto virus* (MRCV) non-structural proteins in insect cells reveals their putative functions. Virology (2012), http://dx.doi.org/10.1016/j.virol.2012.04.016

Roy, P., Noad, R., 2006. Bluetongue virus assembly and morphogenesis. Curr. Top. Microbiol. Immunol. 309, 87–116.
Satoh, K., Shimizu, T., Kondoh, H., Hiraguri, A., Sasaya, T., Choi, I.R., Omura, T., Kikuchi, S., 2011. Relationship between symptoms and gene expression induced by the infection of three strains of Rice dwarf virus. PloS One 6, e18094.
Seo, J., Lee, K.J., 2004. Post-translational modifications and their biological functions: proteomic analysis and systematic approaches. J. Biochem. Mol. Biol. 37, 35–44.
Shikata, E., Kitagawa, Y., 1977. Rice black-streaked dwarf virus: its properties, morphology and intracellular localization. Virology 77, 826–842.
Shimizu, T., Nakazono-Nagaoka, E., Uehara-Ichiki, T., Sasaya, T., Omura, T., 2011. Targeting specific genes for RNA interference is crucial to the development of strong resistance to rice stripe virus. Plant Biotechnol. J. 9, 503–512.
Supyani, S., Hillman, B.I., Suzuki, N., 2007. Baculovirus expression of the 11 mycoreovirus-1 genome segments and identification of the guanylyltransferase-encoding segment. J. Gen. Virol. 88, 342–350.
Wang, Q., Tao, T., Zhang, Y., Wu, W., Li, D., Yu, J., Han, C., 2011. Rice black-streaked dwarf virus P6 self-interacts to form punctate, viroplasm-like structures in the cytoplasm and recruits viroplasm-associated protein P9-1. Virol. J. 8, 24.
Wei, T., Kikuchi, A., Moriyasu, Y., Suzuki, N., Shimizu, T., Hagiwara, K., Chen, H., Takahashi, M., Ichiki-Uehara, T., Omura, T., 2006. The spread of rice dwarf virus among cells of its insect vector exploits virus-induced tubular structures. J. Virol. 80, 8593.
Wei, T., Uehara-Ichiki, T., Miyazaki, N., Hibino, H., Iwasaki, K., Omura, T., 2009. Association of rice gall dwarf virus with microtubules is necessary for viral release from cultured insect vector cells. J. Virol. 83, 10830–10835.
Wu, Z., Wu, J., Adkins, S., Xie, L., Li, W., 2010. Rice ragged stunt virus segment S6-encoded nonstructural protein Pns6 complements cell-to-cell movement of Tobacco mosaic virus-based chimeric virus. Virus Res. 152, 176–179.
Zimmermann, R., Eyrisch, S., Ahmad, M., Helms, V., 2011. Protein translocation across the ER membrane. BBA 1808, 912–924.

Please cite this article as: Maroniche, G.A., et al., *In vivo* subcellular localization of *Mal de Río Cuarto virus* (MRCV) non-structural proteins in insect cells reveals their putative functions. Virology (2012), http://dx.doi.org/10.1016/j.virol.2012.04.016